

1984

# Design of Compressor Suspension Systems Using Modal Analysis

N. Gupta

R. J. Bernhard  
bernhard@purdue.edu

Follow this and additional works at: <https://docs.lib.purdue.edu/icec>

---

Gupta, N. and Bernhard, R. J., "Design of Compressor Suspension Systems Using Modal Analysis" (1984). *International Compressor Engineering Conference*. Paper 447.  
<https://docs.lib.purdue.edu/icec/447>

This document has been made available through Purdue e-Pubs, a service of the Purdue University Libraries. Please contact [epubs@purdue.edu](mailto:epubs@purdue.edu) for additional information.

Complete proceedings may be acquired in print and on CD-ROM directly from the Ray W. Herrick Laboratories at <https://engineering.purdue.edu/Herrick/Events/orderlit.html>

DESIGN OF COMPRESSOR SUSPENSION SYSTEMS  
USING MODAL ANALYSIS

Nishi Gupta\*  
IBM Corporation  
Manassas, Virginia

Robert J. Bernhard, Assistant Professor  
Ray W. Herrick Laboratories  
School of Mechanical Engineering  
Purdue University  
West Lafayette, IN 47907

ABSTRACT

A modal analysis procedure is used to model suspended compressors and their excitation forces. The modal method evaluates the dynamic spring forces, modal spring forces, and modal forcing function to determine the effects of a change in suspension configuration on transmitted spring forces. Valuable design insight is gained since the modal parameters explain the behavior of suspension systems during steady state compressor motion concisely. Also, many suspension configurations can be analyzed due to the cost effectiveness of the modal procedure. A parameter study is done to illustrate an application of the procedure.

NOMENCLATURE

$A_i, B_i$  = unknown coefficients determined by initial conditions  
[C] = 6 x 6 damping matrix  
 $D_{ij}$  = absolute difference between maximum and minimum spring force in direction i during cycle j for new spring configuration  
 $E_{ij}$  = same as  $D_{ij}$  for reference spring configuration  
[F] = 6 x 1 harmonic force vector  
[ $F_s$ ] = 3 x 1 spring force vector  
[I] = identity matrix  
[K] = 6 x 6 stiffness matrix

[M] = 6 x 6 inertial matrix  
{ $M_s$ } = 3 x 1 spring moment vector  
MS = modal spring force  
N = number of springs  
NC = number of cycles  
[P] = eigenvector matrix normalized with respect to [M]  
[ $\bar{P}$ ] = eigenvector matrix  
[S] = 6 x 6 equivalent stiffness matrix for a spring  
{X} = 6 x 1 displacement vector  
n = number of evaluation points  
{p} = normalized eigenvector  
{ $\bar{p}$ } = eigenvector  
{q} = 6 x 1 modal displacement vector  
{s} = stiffness vector, a column in the symmetric [S] matrix  
 $\omega_{DR}$  = forcing function frequency  
 $\omega_i$  = ith natural frequency  
 $\phi_i$  = phase angle between the first and ith forcing function  
 $\beta$  = criteria function  
[ $\Lambda$ ] = 6 x 6 diagonal matrix containing the square of the natural frequencies  
{ $\Gamma$ } = modal force vector  
GMS = modal criteria function

\* work was performed while a Graduate Research Assistant at Ray W. Herrick Laboratories, Purdue University.

## INTRODUCTION

The compressor suspension configuration has a significant effect on transmitted spring forces and compressor vibration as discussed by Kjeldsen and Madsen [1]. Time integration models, which accurately predict steady state compressor motion, can be used to redesign compressor suspension systems by a trial and error procedure [2,3]. However, the time integration models are expensive in terms of computer resources and offer little design insight. In this paper, a modal model is developed and then studied for its feasibility as a model of the forced suspended body problem.

## MODAL MODEL

To develop the modal model, the equations of motion of the suspended compressor, shown in Fig. 1, are first obtained and then decoupled by application of modal principles [4]. The equations of motion are derived from Hamilton's experimentally verified time integration model [2]. Assuming that the compressor behaves as a rigid body, the six equations of motion in matrix form are

$$[M]\{\ddot{X}\} + [C]\{\dot{X}\} + [K]\{X\} = \{F\} \quad (1)$$

Although the damping matrix can be used, the modal model developed in this paper assumes negligible damping such that Eq. (1) is simplified to

$$[M]\{\ddot{X}\} + [K]\{X\} = \{F\} \quad (2)$$

The system stiffness matrix [K] is written as

$$[K] = \sum_{i=1}^N [S]_i \quad (3)$$

where  $[S]_i$  is the equivalent spring stiffness matrix for spring  $i$  at the compressor's center of gravity and  $N$  is the number of springs. The stiffness properties of the discharge tube are approximated as a spring by the finite element method [3]. The spring forces and moments at the compressor's center of gravity due to each spring are

$$\begin{bmatrix} \{F_s\}_i \\ \{M_s\}_i \end{bmatrix} = [S]_i \{X\} \quad i=1, \dots, N. \quad (4)$$

Complete methods for determining [M], [K], and {F} are given by Hamilton [2].

To decouple Eq. (2), the eigenvector matrix [P] is first normalized with respect to [M] by normalizing each eigenvector  $\{\bar{p}\}_i$

$$\{p\}_i = \frac{\{\bar{p}\}_i}{\{\bar{p}\}_i^T [M] \{\bar{p}\}_i} \quad i=1, \dots, 6. \quad (5)$$

Next, the modal principles are applied to Eq. (2). Substituting

$$\{X\} = [P]\{q\}, \quad (6)$$

where {q} is the modal displacement vector, produces the equation

$$[M][P]\{\ddot{q}\} + [K][P]\{q\} = \{F\}. \quad (7)$$

Multiplying Eq. (7) by  $[P]^T$  yields

$$[P]^T [M] [P] \{\ddot{q}\} + [P]^T [K] [P] \{q\} = [P]^T \{F\}. \quad (8)$$

The identities

$$[P]^T [M] [P] = [I] \quad (9)$$

and

$$[P]^T [K] [P] = [\Lambda] \quad (10)$$

are used to reduce Eq. (8) to

$$[I]\{\ddot{q}\} + [\Lambda]\{q\} = \{\Gamma\} \quad (11)$$

where

$$[\Lambda] = \begin{bmatrix} \omega_1^2 & 0 & 0 & 0 & 0 & 0 \\ 0 & \omega_2^2 & 0 & 0 & 0 & 0 \\ 0 & 0 & \omega_3^2 & 0 & 0 & 0 \\ 0 & 0 & 0 & \omega_4^2 & 0 & 0 \\ 0 & 0 & 0 & 0 & \omega_5^2 & 0 \\ 0 & 0 & 0 & 0 & 0 & \omega_6^2 \end{bmatrix} \quad (12)$$

and  $\{\Gamma\}$  is the modal force vector. The six decoupled governing equations of motion can now be solved individually.

When the components of the forcing function are in phase sine functions as shown in Fig. 2, the general solution for Eq. (11) is

$$q_i = \frac{\Gamma_i (\sin \omega_{DR} t + \phi_i)}{\omega_i^2 - \omega_{DR}^2} + A_i \sin \omega_i t + B_i \cos \omega_i t.$$

$A_i$  and  $B_i$ , which are dependent on the compressor's free response and initial conditions, are assumed to be negligible compared to  $\Gamma_i$  at steady state. Also, this assumption simplifies the model if initial conditions are not known. Thus, Eq. (13) is reduced to

$$q_i = \frac{\Gamma_i}{\omega_1^2 - \omega_{DR}^2} \quad i=1, \dots, 6 \quad (14)$$

When the forcing function is complex as shown in Figs. 3 and 4, Eq. (14) may be evaluated by setting  $\Gamma_i$  as the summation of the Fourier components of the  $i$ th modal forcing function. A simpler and reasonably correct alternative is to evaluate the modal forcing function at various times during one cycle of the harmonic forcing function. With the simpler approach, enough points are used to insure that the combinations of forces and moments which result in the worst spring force case are obtained. The variable  $\Gamma_i$  in Eq. (14) corresponds to the value of the  $i$ th modal forcing function at the evaluation step  $j$ . This solution technique is written as

$$q_{ij} = \frac{\Gamma_{ij}}{\omega_1^2 - \omega_{DR}^2} \quad \begin{matrix} i=1, \dots, 6 \\ j=1, \dots, n \end{matrix} \quad (15)$$

where  $n$  equals the number of evaluation points in one cycle of the harmonic forcing function. The choice of  $n$  is arbitrary and the points need not be uniformly distributed over one cycle.

With  $\{q\}$  evaluated, the spring forces and moments for each spring are found by substituting Eq. (6) into Eq. (4)

$$\begin{Bmatrix} F_s \\ M_s \end{Bmatrix}_i = [S]_i [P] \{q\} \quad i=1, \dots, N \quad (16)$$

Only the spring forces,  $\{F_s\}_i$ , are discussed in this paper.

#### CRITERIA FUNCTION

Because  $A_i$  and  $B_i$  were assumed to be negligible in Eq. (13),  $q_i$  will not be exact, and the spring forces obtained with the modal model will not correspond exactly with the spring forces obtained with the time integration model. Hence, monitoring the maximum spring forces for various spring configurations will not produce exact correlation between the two models.

However, the modal model does accurately predict the average dynamic spring forces at steady state. A criteria function,  $\beta_i$ , which computes a statistical average of the ratios of the dynamic spring forces for two spring configurations can be developed such that

$$\beta_i = \frac{\sum_{j=1}^{NC} \frac{D_{ij}}{E_{ij}}}{NC} \quad \begin{matrix} i=1, \dots, 3 \\ j=1, \dots, NC \end{matrix} \quad (17)$$

where  $NC$  equals the number of cycles. For the modal model,  $NC$  equals one. For the time integration model, the value of  $NC$  is

arbitrary. In Eq. (17),  $D_{ij}$  is the absolute difference between maximum and minimum spring force in direction  $i$  during cycle  $j$  for a new spring configuration.  $E_{ij}$  is the same as  $D_{ij}$  evaluated for the reference spring configuration.

#### VERIFICATION OF MODAL MODEL

To determine the accuracy of the modal model, the  $\beta$  values obtained with the modal model are compared to those obtained with Hamilton's experimentally verified time integration model. Three spring configurations, shown in Figs. 5 and 6, are used for the verification procedure. Spring configuration A, the original spring configuration, is taken to be the reference configuration for the  $\beta$  calculations in Eq. (17). In configuration B, the springs are located such that the compressor's center of gravity coincides with the center of the area formed by the suspension springs in the  $x$ - $y$  plane. Configuration C is the same as B except that the spring mounting points are now on the compressor's center of gravity plane. The position of the discharge tube is not changed for any of the configurations studied.

To analyze the effects of different forcing functions on the accuracy of the modal model, two test cases are used. The first test case involves a simple forcing function as shown in Fig. 2, and the second test case consists of a complicated forcing function as shown in Figs. 3 and 4.

#### Case 1

For case 1, the shaking forces are idealized such that

$$F_x = F_z = M_y = M_z = 0 \quad (18)$$

and  $F_y$  and  $M_x$  are as shown in Fig. 2. Table 2 lists the  $\beta$  values for spring configurations B and C where the theoretical  $\beta$  values are obtained with the modal model and the actual  $\beta$  values are obtained with the time integration model. As shown in Table 2, the correlation between theoretical and actual  $\beta$  values is excellent. For configuration C, which is a significant change in the suspension system, the error between the theoretical and actual  $\beta$  values ranges from 0% to only 1.6%.

#### Case 2

For case 2, the force vector includes the shaking forces, shaking moments, and gyroscopic moments associated with the compressor. Fig. 3 shows the harmonic forces normalized with respect to the magnitude of  $F_y$ , and Fig. 4 shows the harmonic moments normalized with respect to the magnitude of  $M_x$ .

The  $\beta$  values listed in Table 2 show that the correlation between theoretical and actual values is not as accurate as for case 1. However, the results are still acceptable as an indicator of the changes in spring forces. For example, the theoretical and actual  $\beta_y$  values for configuration C indicate that the largest percentage of reduction in spring force occurs for the y spring force for all four springs.

Tables 1 and 2 show the importance of an accurate forcing function. The  $\beta$  values obtained with the simple forcing function are not the same as the values evaluated with the complex forcing function. Thus, to correctly analyze a suspension configuration, a reasonable approximation of the forcing function should be used. For the remaining analysis, only the complicated forcing function (case 2) is utilized.

#### PARAMETER STUDY

Parameter studies can be efficiently done with the modal model. To illustrate a parameter study, the effects of the spring mounting plane on the spring forces for spring 2 are analyzed. The  $\beta$  values in Fig. 7 indicate that the springs should be mounted at the compressor's center of gravity plane to obtain the minimum value of  $\beta_x$  and  $\beta_y$  for spring 2. As shown in Figs. 1 and 5, the original spring mounting plane is below the compressor's center of gravity. The results in Fig. 7 agree with the work done by Kjeldsen and Madsen [1] on reduction of compressor vibrations. Kjeldsen and Madsen concluded that in order to minimize horizontal spring displacements the spring mounts and the cylinder axis should be on opposite sides of the compressor's center of gravity plane.

Fig. 7 also reveals that a variation in the z location of the spring mounting plane has little or no effect on the transmitted spring force in the z direction. This result agrees with Kjeldsen and Madsen's findings that the vertical location of the spring mounting plane does not effect the vertical displacements of the springs.

#### DESIGN ANALYSIS

The modal model is a simplified simulation of the compressor suspension and can be used to obtain insight for the design of compressor suspension systems. To determine how a suspension configuration effects transmitted spring forces, the following three terms are monitored:

1. magnitude of the modal forcing function,  $\Gamma$
2. modal spring force, MS and
3. modal criteria function,  $\Gamma MS$ .

$\Gamma$  shows the extent of excitation of a mode by the forcing function  $\{F\}$ . From Eqs. (8) and (11),  $(\Gamma)_j$  which is the absolute largest value of the jth modal forcing function can be expressed as

$$(\Gamma)_j = \{p\}_j^T \{F\} \quad j=1, \dots, 6 \quad (19)$$

where  $\{p\}_j$  is the jth eigenvector. MS indicates the effect of a mode shape on a spring force. From Eq. (16), the spring forces for one spring are

$$\begin{bmatrix} \{F_s\} \\ \{M_s\} \end{bmatrix} = [S] [P] \{q\}. \quad (20)$$

In terms of the modal spring force matrix  $[MS]$ , Eq. (20) becomes

$$\begin{bmatrix} \{F_s\} \\ \{M_s\} \end{bmatrix} = [MS] \{q\} \quad (21)$$

where

$$[MS] = [S][P] \quad (22)$$

and  $\{q\}$  is defined in Eq. (15). A modal spring force in force direction i due to mode j is

$$(MS)_{ij} = \{s\}_i^T \{p\}_j \quad \begin{matrix} i=1, \dots, 6 \\ j=1, \dots, 6 \end{matrix} \quad (23)$$

where  $\{s\}_i$  is the ith column in the symmetric stiffness matrix  $[S]$ . The modal criteria function is the product of  $\Gamma$  and MS and is expressed as

$$(\Gamma MS)_{ij} = (\Gamma)_j (MS)_{ij} \quad \begin{matrix} i=1, \dots, 6 \\ j=1, \dots, 6 \end{matrix} \quad (24)$$

The modal criteria function indicates the combined effects of the driving force and mode shape on the spring force.

For a typical design procedure, the direction of important spring force is determined first. Next, the critical modes for each configuration are determined and the  $\Gamma MS$  values corresponding to the critical modes are compared. To illustrate this procedure, the spring force in the y direction for spring 2 is analyzed. Table 3 lists the corresponding  $\Gamma$ , MS, and  $\Gamma MS$  values. Also, Table 4 lists the  $\{s\}_i$  and  $\{p\}_j$  vectors for a selected mode for each configuration.

The critical modes are the modes with the large  $\Gamma MS$  values. For configuration A, mode 6 is the critical mode as evident by the large  $\Gamma MS$  value. Mode 5 is the critical mode for configuration B. Although there are no dominant modes for configuration C, modes 1, 2, 3, and 6 are considered to be the critical modes.

Mode 5 for configuration B and mode 6 for configuration A are suspected to have similar characteristics because the  $\Gamma$ , MS, and  $\Gamma MS$  values for the two modes are similar. Table 4 shows that both  $\{p\}_6$  for con-

figuration A and  $\{p\}_5$  for configuration B have the largest displacement in the y direction and the largest rotation in the x direction. Also, the stiffness vectors  $\{s\}_2$  for both configurations are similar.

The lack of reduction in  $\Gamma$ MS values of the critical modes between configuration A and configuration B indicates that the y spring force is not reduced with configuration B. As shown in Figs. (3) and (4), the largest force is  $F_y$  and the largest moment is  $M_x$ . For configuration B, the mode shape  $\{p\}_5$  has the largest displacement in the y direction and the largest rotation in the x direction. Thus, mode 5 is strongly excited by the forcing function  $\{F\}$  because the directions of the largest forces coincide with the largest displacements of the mode shape.

With configuration C, the effect of mode 4 on the spring force has been minimized although  $\Gamma$  for mode 4 has not decreased significantly in comparison to  $\Gamma$  for mode 6 in configuration A. As shown in Table 4, mode 4 for configuration C,  $\{p\}_4$ , has the largest displacement in the y direction and the largest rotation in the x direction. Thus, mode 4 is strongly excited by the forcing function  $\{F\}$  as discussed earlier. However, the large  $\Gamma$  is counteracted by a substantial reduction in MS. By moving the spring mounting plane up to the compressor's center of gravity, the stiffness term corresponding to a rotation around the x axis has been eliminated in  $\{s\}_2$ . Hence, moments about the x axis do not result in a large transmitted spring force in the y direction for configuration C.

For configuration C, the  $\Gamma$ MS values for the critical modes have decreased by at least 75% in comparison with the largest  $\Gamma$ MS value for configuration A. The large reduction indicates that configuration C improves the y spring force for spring 2. The modal analysis correlates with the theoretical  $\beta_y$  of 0.303 evaluated for configuration C.

The modal analysis shows that in order to reduce spring forces  $\Gamma$ MS has to decrease by a reduction in either  $\Gamma$  and/or MS. To reduce  $\Gamma$ , the suspension configuration should be designed such that the modes are not excited by the forcing function  $\{F\}$ . To reduce MS, the stiffness properties in the directions corresponding to large modal displacements should be minimized. Although it may not be possible to eliminate the effects of critical modes, it is possible to understand and possibly minimize the effects of critical modes by application of fundamental modal analysis principles [5].

## CONCLUSIONS

The studies done in this paper show that the modal model is an accurate method for steady state analysis of suspension configurations. The modal model also reduces the computer costs associated with the time integration model by 80%. With the modal information, insight is gained for the improvement of suspension configurations. Also, the modal model is more general than previous design models [1] because the modal model can include all of the excitation forces associated with the compressor. Thus, the modal model has proven to be an efficient design tool.

## REFERENCES

- [1] Kjeldsen, K. and Madsen, P., "Reduction of Compressor Vibrations by Optimizing the Locations of the Counterweight and the Internal Springs," Proceedings of the 1978 Purdue Compressor Technology Conference.
- [2] Hamilton, J.F., Modeling and Simulation of Compressor Suspension System Vibrations, Purdue University, West Lafayette, Indiana, 1982.
- [3] Jenkins, S.T., "Reduction of Transmitted Vibration Forces Through the Support Springs of a Compressor," MSME Thesis, Purdue University, West Lafayette, Indiana, 1980.
- [4] Meirovitch, L., Elements of Vibration Analysis, New York: McGraw-Hill, 1975.
- [5] Soedel, W., Vibrations of Shells and Plates, Marcel Dekker, Inc., 1981.

Table 1.  $\beta$  values for spring configurations B and C (case 1).

	Configuration B		Configuration C	
	Theoretical	Actual	Theoretical	Actual
Spring 1				
$\beta_x$	1.375	1.400	4.760	4.836
$\beta_y$	0.995	0.996	0.466	0.468
$\beta_z$	0.923	0.920	0.900	0.898
Spring 2				
$\beta_x$	1.375	1.400	4.760	4.836
$\beta_y$	0.995	0.996	0.472	0.474
$\beta_z$	0.923	0.922	0.901	0.899
Spring 3				
$\beta_x$	0.834	0.837	0.353	0.354
$\beta_y$	0.994	0.996	0.472	0.474
$\beta_z$	0.697	0.696	0.679	0.679
Spring 4				
$\beta_x$	0.834	0.837	0.353	0.354
$\beta_y$	0.995	0.997	0.466	0.469
$\beta_z$	0.702	0.701	0.684	0.684

Table 2.  $\beta$  values for spring configurations B and C (case 2).

	Configuration B		Configuration C	
	Theoretical	Actual	Theoretical	Actual
Spring 1				
$\beta_x$	0.955	0.940	0.454	0.576
$\beta_y$	0.989	0.980	0.327	0.263
$\beta_z$	0.935	0.917	0.921	0.872
Spring 2				
$\beta_x$	0.955	0.940	0.454	0.576
$\beta_y$	0.991	0.981	0.303	0.212
$\beta_z$	0.934	0.922	0.920	0.881
Spring 3				
$\beta_x$	1.013	1.039	1.747	1.794
$\beta_y$	0.989	0.981	0.303	0.212
$\beta_z$	0.746	0.723	0.735	0.688
Spring 4				
$\beta_x$	1.013	1.039	1.747	1.794
$\beta_y$	0.985	0.978	0.326	0.263
$\beta_z$	0.744	0.732	0.732	0.700

Table 3. Modal data and RMS values in y direction for spring 2  
(case 2)

	Mode Number					
	1	2	3	4	5	6
Config. A						
Γ	916.4	228.5	223.0	755.1	639.9	1958.0
MS	32.6	382.6	137.0	521.7	186.4	919.5
ΓMS	29,875	87,424	30,551	393,936	119,277	1,800,381
Config. B						
Γ	931.9	365.9	722.7	5.1	1958.0	656.5
MS	15.2	291.7	502.2	5.8	968.6	155.2
ΓMS	14,165	106,733	362,940	30	1,896,519	101,889
Config. C						
Γ	646.4	613.3	764.1	1854.0	127.6	869.3
MS	422.4	542.1	262.5	0.8	74.7	497.5
ΓMS	273,039	332,470	200,576	1,483	9,532	432,477

Table 4. {s} and {p} for a selected mode for each configuration  
(spring 2 y-force)

Configuration A		Configuration B		Configuration C	
{s} <sub>2</sub>	{p} <sub>6</sub>	{s} <sub>2</sub>	{p} <sub>5</sub>	{s} <sub>2</sub>	{p} <sub>4</sub>
0	-.0058	0	-.0034	0	-.0045
1579	-.1564	1579	.2025	1579	.0202
0	-.0515	0	.0011	0	-.0065
6938	-.0939	6938	.0898	0	.1002
0	.0037	0	.0006	0	-.0162
-5684	.0037	-5527	-.0046	-5527	.0056

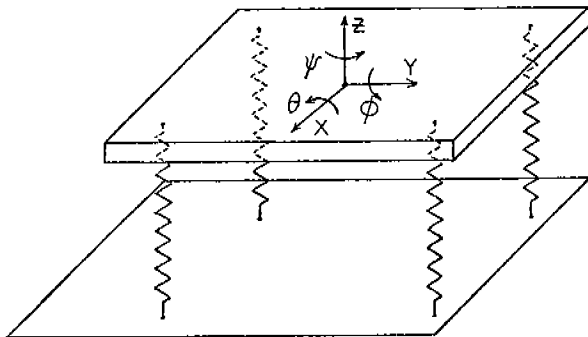


Figure 1 Schematic of suspended compressor

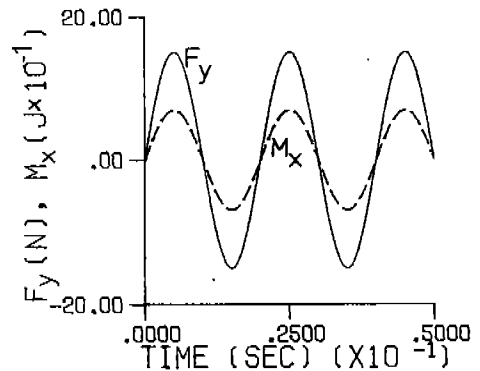


Figure 2  $F_y$  and  $M_x$  for Case 1



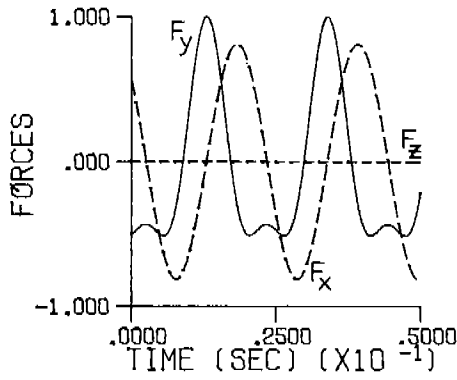


Figure 3 Normalized forces for Case 2

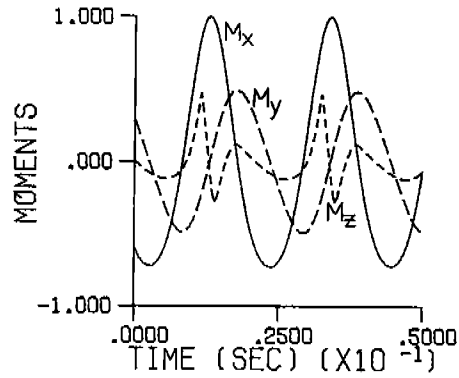
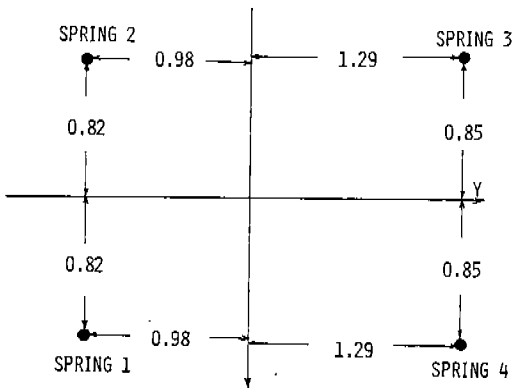
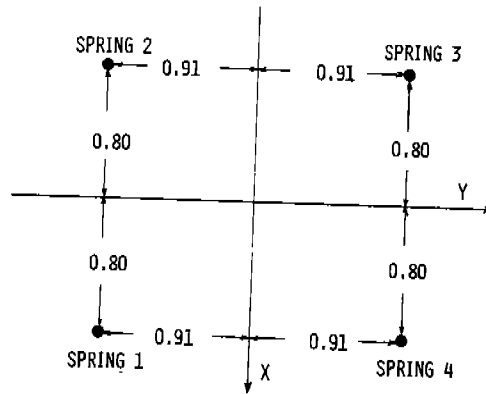


Figure 4 Normalized moments for Case 2



SPRING CONFIGURATION A:  $Z = -1.0$

Figure 5 Spring Configuration A



SPRING CONFIGURATION B:  $Z = -1.0$

SPRING CONFIGURATION C:  $Z = 0.0$

Figure 6 Spring Configuration B and C

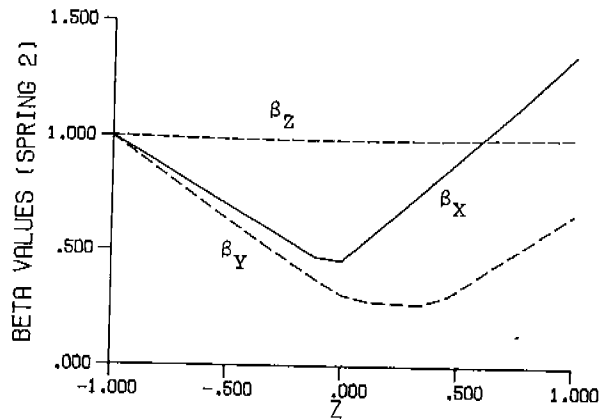


Figure 7  $\beta$  values as functions of  $Z$  for spring 2